Optimal sizing and sensitivity analysis of a battery-supercapacitor energy storage system for electric vehicles

Tao Zhu [a,*], Richard G. A. Wills [a], Roberto Lot [a,b], Xiaodan Kong [c], Xingda Yan [d]

[a] *Department of Mechanical Engineering, University of Southampton, Southampton, SO17 1BJ, UK.*
[b] *Department of Industrial Engineering, University of Padova, Padova, 35131, Italy.*
[c] *Glorious Sun School of Business and Management, Donghua University, Shanghai, 200051, China.*
[d] *Compound Semiconductor Applications Catapult, Newport, NP10 8BE, UK*
[*] *Corresponding author: T.Zhu@soton.ac.uk* (*T. Zhu*).

Abstract: This paper presents a sizing method with sensitivity analysis for battery-supercapacitor hybrid energy storage systems (HESSs) to minimize vehicle-lifetime costs. An optimization framework is proposed to solve joint energy management-sizing optimization. Sensitivity analysis is performed using eight parameters of the vehicle, HESS system and components as sensitive factors. We explain why HESS sizing is sensitive to each factor by discussing the change of optimal HESS size and costs with varying factor values. The relative importance of each factor in practical engineering is quantified and compared. Results show that battery degradation accounts for around 89% of HESS costs; among eight sensitive factors, vehicle driving range has the biggest impact on HESS costs with a calculated impact degree of 1.243. By analyzing comprehensive factors in optimization of HESS sizing, it is expected to provide general a sizing guide applicable to various application scenarios of HESS in electric vehicles.

Keywords: Electric vehicle**,** Hybrid energy storage system, Cost optimization, Sizing, Sensitivity analysis.

1. Introduction

The electric vehicle (EV) market is projected to reach 27 million units by 2030 from an estimated 3 million units in 2019 [1]. Demands of energy-efficient and environment-friendly transportation usher in a great many of energy storage systems (ESSs) being deployed for EV propulsion [2]. The onboard ESS is expected to have a high energy capacity to sustain long-distance driving, as well as a high power capability to enable sharp accelerations and regenerative braking. Batteries, which are the most popular ESSs in EVs, are capable of

delivering long-term driving energy, but less suited for satisfying short-term power loads experienced in rapid acceleration and regenerative braking deceleration [3]. To sustain high power loads, battery-only ESSs are usually heavy with a large volume [4]. In other words, other technologies or separate battery systems may provide performance benefits when used to offer high power pulses without degradation, particularly of the main range providing energy store [5]. One possible solution to supplementing the performance limitations of batteries is to deploy supercapacitors (SCs) as the second energy storage device working with batteries [6]. As a complementary option for batteries, SCs feature high-transient, efficient power capability over millions of full-charge cycles [7]. SCs unload batteries by peaking bursts of power demands while requiring only the average power from batteries [8]. In combination, the advantages of battery-SC hybrid energy storage system (HESS) should outweigh the performance of either storage technology acting alone [4]. Previous research has already reported that HESSs reduce energy consumption and battery degradation as compared with battery-only ESSs [6].

The battery-SC HESS comprises one battery pack, one SC pack and one (or multiple) DC/DC converter(s); therefore, the size of a battery-SC HESS can be determined by solving for the above components [9]. However, sizing is not limited to specifying the physical dimension of each HESS component; instead, sizing often incorporates specific objectives as optimization problems. As such, minimizing electricity consumption or energy storage degradation is the commonly investigated objective of sizing [10]. Targeted conflicting optimization objectives from different metrics, multi-objective optimization (MOP) is a popular method for HESS analysis. For example, in [11], a MOP problem is proposed for sizing a HESS applied in a passenger EV with two objectives of mass and battery cycle life, while the Pareto front of the size of HESS is obtained via the DIRECT algorithm. In [12], HESS sizing is studied in a prototype EV, and a MOP problem is proposed with optimization of battery health, HESS mass and financial costs; the optimal HESS size is solved by the non-dominated sorting genetic algorithm II and wavelet-transform-based algorithm. In this paper, the authors set up four objectives: (1) SC purchase cost, (2) DC/DC converter purchase cost, (3) battery degradation cost and (4) HESS energy consumption cost (i.e., the electricity cost consumed by vehicle operations). These objectives are unified into the same metric - financial costs, and the final objective is the overall costs added up by each objective over vehicle lifetime, so that the optimal solution comes from the least overall costs. The definition of objectives will be presented in Section 2.1.

With this approach, this paper optimizes the predefined objectives by the sizing efforts; however, these objectives are affected by not only sizing but also energy management (EM) [10]. Therefore, only looking at sizing while ignoring EM might lead to unfair sizing results. In this regard, EM and sizing problems are always co-investigated. For example, Masih-Tehrani [13] focuses on not only the sizing but also EM for a HESS of an electric bus; aiming at long-term battery replacement cost, the EM is optimized by dynamic programming (DP) while the sizing by genetic algorithm. Song [14] studies an electric bus equipped with a HESS and proposes a joint EM-sizing approach based on DP and rule-based controllers to solve the lifetime financial cost of the HESS. This paper formulates an optimization framework to solve both the EM and size of a HESS with the overreaching goal of minimizing the financial costs of HESS throughout vehicle lifetime. The DP approach is adopted as the solver because of its capability of performing global optimization [15], and is tailored in a three-dimensional form with HESS EM accounting for one dimension and HESS size accounting for two dimensions (because HESS size is reflected by the size of both battery and SC pack). DP is an offline technique that requires prior knowledge of all the input profiles, due to which, DP can hardly be implemented as real-time EM algorithms [16]. However, this paper does not aim at designing a real-time EM strategy that can be used online, but focuses on the sizing problem. In this case, the input profiles for HESS sizing can be known beforehand, so that HESS sizing optimization can be fulfilled by the DP approch offline. The optimization framework based on the DP approach will be presented in Section 2.2. The state-space representation of the HESS used to implement the optimization framework is presented in the appendix.

Combining the objectives and optimization framework, Section 3 presents the optimal sizing results from a set of base-case inputs such as specifications of the EV and HESS components, while the trends of overall costs with HESS size are also discussed. However, even a small change in one of the inputs can lead to very different sizing results. For example, previous research [10] indicates that HESS size and financial costs are quite sensitive to motor efficiency. In [17] the intensity of vehicle driving cycle is found to have a big impact on the optimal SC pack size. In [14] the battery unit price is shown to significantly impact the financial costs and thus influences the optimal sizing results. Therefore, it is necessary to investigate how the optimal sizing results evolve with different inputs, rather than merely offering results for a specific set of inputs. Published articles rarely investigate the influences of different inputs on HESS sizing results; for those performing the investigations, there are limitations as summarized below. Firstly, the categories of investigated inputs can be expanded. In [10, 14,

17], only motor efficiency, vehicle driving cycle and battery unit price are investigated, respectively; however, other inputs such as vehicle driving range and HESS topology, which may have significant impacts on HESS sizing results [18], have not been taken into consideration. Secondly, although the impacts of investigated inputs are worked out, these articles lack discussion on the in-depth reasons for causing the impacts. It is still ambiguous why the sizing results are sensitive to the investigated inputs. Lastly, each article investigates specific inputs separately but fails to present a clear parallel comparison among different inputs. Therefore, the relative importance of different inputs is not clear, and each article only stresses the impacts of the specifically investigated inputs. Considering a comprehensive study on different inputs is still a missing part of HESS research, this paper performs sensitivity analysis towards eight categories of inputs (i.e. sensitive factors): vehicle driving cycle, vehicle driving range, HESS topology, nominal bus voltage, DC/DC conversion efficiency, component price (further divided into battery price, SC price and DC/DC converter price). These sensitive factors are classified into three levels, as Fig. 1, while the reasons for choosing these factors are due to their significance to vehicle dynamic performance, HESS architecture, component selection, and that they are usually considered at early-stage vehicle development [19]. To understand whether and why HESS sizing is sensitive to these factors, the trends of optimal HESS size and overall costs with varying sensitive factors, as well as the underlying causes of the trends, are discussed in Section 4. More than that, this paper also tries to identify the impact degrees of sensitive factors so that the importance of each factor can be distinguished for guiding practical engineering; namely, the factors with high impact degrees need more consideration in practice while those with low impact degrees may be sacrificed since it is difficult to focus on every sensitive factor. The impact degrees of different factors will be presented in Section 5.

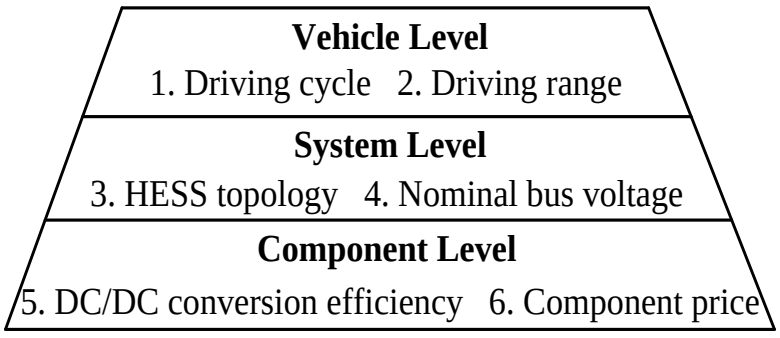

Fig. 1. Sensitive factors in the vehicle, system and component levels.

Based on the above, this paper presents an optimal sizing method with sensitivity analysis specifically for the HESS deployed in light passenger EVs to minimize financial costs over vehicle lifetime, with the following contributions. Finally, the conclusion will be drawn in Section 6.

(1) The HESS sizing method to optimize financial costs over vehicle lifetime is proposed. The optimization problem is solved by a joint EM-sizing optimization framework based on a three-dimensional DP approach.

(2) A sensitivity analysis of optimal HESS size and financial costs is performed on various sensitive factors. The underlying reasons for these factors to cause sensitivity are discussed. The relative importance of each sensitive factor is identified, which can guide the trade-off among factors in practical engineering.

2. HESS sizing method

The size of HESS is reflected by two design variables, the size of battery pack (in kWh) and the size of SC pack (in Wh). This paper does not consider the DC/DC converter size as a design variable because it depends on the size of either battery or SC pack [20]. The final objective of HESS sizing is the overall financial costs of HESS over vehicle lifetime, which is divided into four kinds of sub-costs. This section defines the sub-costs and formulates the DP-based optimization framework to find the optimal HESS size that can minimize overall costs. The state-space representation of HESS, which is associated with the optimization framework, is presented in the appendix.

2.1 Definition of financial costs

The overall financial costs of HESS should cover the costs from initial deployment to long-term service until the vehicle lifetime expires. The costs that happen with HESS initial deployment are the initial costs; in this paper, the initial costs are considered as the money to purchase each HESS component. The costs that accumulate with HESS long-term service are the long-term costs; this paper considers that the long-term costs come from the component replacements caused by component degradation and the energy consumption by HESS operations. Among HESS components, the SC pack and DC/DC converter are regarded as having long enough lifespan and no replacements over vehicle lifetime [21], thus they have one-off purchase costs but no degradation cost. For the battery pack, it has not only the purchase cost but also the degradation cost because battery lifespan can be shorter than vehicle lifetime, and the battery pack may be replaced for several times over vehicle lifetime [22]. In this paper,

the battery purchase cost is regarded as equivalent to the battery degradation cost that happens with first-time battery replacement. Therefore, the battery purchase cost is merged into battery degradation cost and counted into long-term costs. Besides, HESS operations consume an amount of energy, and the corresponding energy cost over vehicle lifetime is counted into long-term costs. Based on the above, Fig. 2 shows the overall costs composed of four kinds of sub-costs.

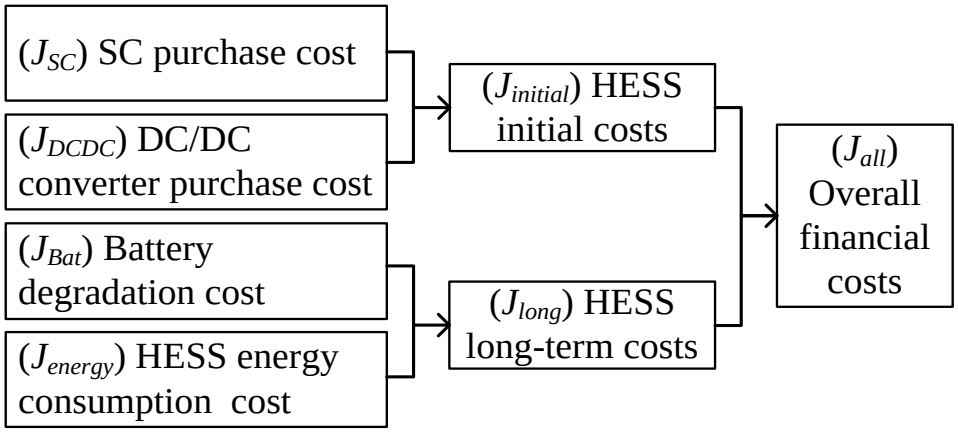

Fig. 2. Division of overall financial costs of HESS over vehicle lifetime.

SC purchase cost (J_{SC}) is calculated as directly proportional to the energy capacity of SC pack, as Eq. (1), where $Price_{SC}$ is the SC unit price in USD/Wh, E_{SC} is the energy capacity of SC pack in Wh and used to express SC pack size and is solved by the sizing efforts of the optimization framework.

$$J_{SC} = Price_{SC} E_{SC} \tag{1}$$

DC/DC converter purchase cost (J_{DCDC}) is calculated as directly proportional to the rated power capability of DC/DC converter ($P_{DCDC,\ rated}$, in kW, it is used to represent DC/DC converter size). $P_{DCDC,\ rated}$ depends on the maximum working power of either battery or SC pack, whichever interfaced by the DC/DC converter [18], as Eq. (2), where $Price_{DCDC}$ is the DC/DC converter unit price in USD/kW, $P_{BAT,max}$ and $P_{SC,max}$ are the maximum working power of battery and SC pack in kW, respectively, and they are solved by the EM efforts of the optimization framework.

$$J_{DCDC} = Price_{DCDC} P_{DCDC,rated}, \quad P_{DCDC,rated} = \begin{cases} P_{BAT,max} \\ or \\ P_{SC,max} \end{cases} \tag{2}$$

Battery degradation cost (J_{BAT}) is calculated as directly proportional to the energy capacity loss of battery pack ($E_{BAT,loss}$, the lost energy capacity due to battery degradation, in kWh). As compared with J_{SC} and J_{DCDC} that happen only once and then remain unchanged over vehicle lifetime, J_{BAT} increases as $E_{BAT,loss}$ grows with HESS operations [23]. Eq. (3) uses the $E_{BAT,loss}$ in the period of single driving cycle to assess the J_{BAT} throughout vehicle lifetime. In Eq. (3), a coefficient of 20% is divided by because as each time $E_{BAT,loss}$ reaches 20% of the original energy capacity of battery pack, the entire battery pack is commonly recognized as end-of-life and loses all its values, in which case battery replacement happens [24]. $Price_{BAT}$ is battery unit price in USD/kWh. $Range_{vehiclelife}$ represents the vehicle mileage when vehicle lifetime is considered to expire [25], while $Range_{drivecycle}$ represents the distance of single driving cycle in km, therefore, ($Range_{vehiclelife}$/$Range_{drivecycle}$) transfers the battery degradation cost of single driving cycle to those of vehicle lifetime. $E_{BAT,loss}$ can be further expressed as the product of original energy capacity of battery pack (E_{BAT}, in kWh, used to express the size of battery pack and solved by sizing efforts of the optimization framework) and battery degradation coefficient (α, in %, expressed as $E_{BAT,loss}$ divided by E_{BAT}) [26], as Eq. (4). The calculation of α adopts a derived formula from [27], as Eq. (5), where I_{rate} is battery current rate that is expressed as the current of battery (I_{BAT}, in A, solved by the equivalent circuit model) divided by the Ah capacity of battery (C_{BAT}, in Ah), $Ah_{throughput}$ is battery ampere-hour throughput that is defined as I_{BAT} multiplied by time t in hour.

$$J_{BAT} = E_{BAT,loss} / 20\% \cdot Price_{BAT} \cdot Range_{vehiclelife} / Range_{drivecycle} \tag{3}$$

$$E_{BAT,loss} = E_{BAT}\alpha \tag{4}$$

$$\begin{cases} \alpha = \dfrac{1}{2364} exp\left(\dfrac{I_{rate}}{2525} \right) Ah_{throughput} \\ I_{rate} = \dfrac{I_{BAT}}{C_{BAT}} \\ Ah_{throughput} = I_{BAT} t \end{cases} \tag{5}$$

HESS energy consumption cost (J_{energy}) is considered as resulting from the energy consumption in the battery pack (Q_{BAT}, in kWh) and SC pack (Q_{SC}, in Wh). Further considering that electricity price is 0.1USD/kWh [28], J_{energy} can be expressed as Eq. (6), which uses HESS energy consumption cost of one driving cycle to evaluate that of vehicle lifetime [29]. Q_{BAT}

and Q_{SC} can be expressed as Eq. (7), where ΔSOC and ΔSOE are the delta state of charge (SOC) of battery pack and the delta state of energy (SOE) of SC pack [30], respectively; SOC is solved by the equivalent circuit model while SOE is solved by the optimization framework.

$$J_{energy} = \left(Q_{BAT} + Q_{SC} / 1000\right) \cdot 0.1USD / kWh \cdot Range_{vehiclelife} / Range_{drivecycle} \quad (6)$$

$$\begin{cases} Q_{BAT} = E_{BAT} \Delta SOC \\ Q_{SC} = E_{SC} \Delta SOE \end{cases} \quad (7)$$

The overall financial costs of HESS over vehicle lifetime (J_{all}) are the sum of all four sub-costs, as Eq. (8), where HESS initial costs ($J_{initial}$) are represented by J_{SC} plus J_{DCDC}, and HESS long-term costs (J_{long}) are represented by J_{BAT} plus J_{energy}.

$$J_{all} = J_{initial} + J_{long} = J_{SC} + J_{DCDC} + J_{BAT} + J_{energy} \quad (8)$$

2.2 Optimization framework based on the DP approach

This section tailors the DP approach as an optimization framework. The outcomes of optimization are to find both the optimal HESS size (represented by the combination of E_{BAT} and E_{SC}) and optimal EM (represented by the SOE of SC pack with time) that can minimize overall costs. The optimization is a six-step process, as described below.

(1) Import profiles. The optimization framework accepts prescribed vehicle parameters (e.g., driving range), HESS architecture (e.g., HESS topology) and HESS component parameters (e.g., battery price) as inputs. As mentioned previously, these inputs are also sensitive factors to be investigated in Section 4.

(2) Traverse HESS sizes in the feasible set. HESS size is processed prior to EM because specific HESS size calls for particularly matched EM to work together and subsequently minimizes overall costs. The optimization process traverses the possible HESS sizes in a feasible set that is constrained by the energy and power requests from vehicle propulsion, as Eqs. (9) and (10). Eq. (9) describes that battery pack energy capacity should satisfy energy requests over vehicle driving range (E_{veh}, in kWh, can be derived from vehicle specifications). Eq. (10) describes that the rated power capability of battery pack ($P_{BAT,rated}$, in kW) and that of SC pack ($P_{SC,rated}$, in kW) together should satisfy the maximum vehicle power request ($P_{veh,max}$, in kW, depends on vehicle parameters and the driving cycle used), where ρ_{BAT} and ρ_{SC} are the power-to-energy density of the battery in 1/hour and that of the SC in 1000/hour, respectively. Combining Eqs. (9) and (10), the minimum allowable energy capacity of battery pack ($E_{BAT,min}$,

in kWh) and SC pack ($E_{SC,min}$, in Wh) can be acquired. Besides, the maximum allowable limits of E_{BAT} and E_{SC} are enforced as $2E_{BAT,min}$ and $10E_{SC,min}$, respectively, in case that the traversal of HESS sizes becomes divergent [31].

$$E_{BAT} \geq E_{veh} \tag{9}$$

$$P_{BAT,rated} + P_{SC,rated} = E_{BAT}\rho_{BAT} + E_{SC}\rho_{SC} \geq P_{veh,max} \tag{10}$$

(3) Traverse EM strategies with time. For each feasible HESS size in the previous step, the optimization process further traverses the possible EM strategies of HESS. EM strategies are time dependent, and the timeline (k) of EM strategies is also the timeline of the input driving cycle [32]. Given that the duration of the input driving cycle is from 0 to t_{end} seconds, the EM strategies can be regulated to perform every one second; thus, k can be expressed as Eq. (11).

$$k = 0,1,2,...,t_{end} \tag{11}$$

At each time point of k, the EM strategies determine the working power of battery pack (P_{BAT}, in kW) and SC pack (P_{SC}, in kW), which are constrained as Eq. (12) and connected as Eq. (13), where P_{veh} is vehicle power request in kW and can be solved from vehicle parameters; η_{DCDC} is the conversion efficiency of DC/DC converter.

$$\begin{cases} \left|P_{BAT}(k)\right| \leq P_{BAT,rated} \\ \left|P_{SC}(k)\right| \leq P_{SC,rated} \end{cases} \tag{12}$$

$$P_{BAT}(k) = \begin{cases} P_{veh}(k) - P_{SC}(k)\eta_{DCDC}, & P_{SC}(k) > 0 \\ P_{veh}(k) - P_{SC}(k)/\eta_{DCDC}, & P_{SC}(k) \leq 0 \end{cases} \tag{13}$$

(4) Calculate electrical states of HESS components. As P_{BAT} and P_{SC} change with time, the electrical states (e.g., voltage, current, SOC, SOE) of HESS components would change as a result. Equivalent circuit models [33] are adopted to account for the change of electrical states. In particular, the SOC of battery pack and SOE of SC pack are constrained as Eq. (14), where SOE_{min} is the minimum allowable SOE, which depends on HESS topology [18] and will be further explained in Section 4.3. Either battery SOC or SC SOE can be used as a state variable (x) to represent the EM states of the HESS, and this paper adopts the later one, as Eq. (15), where SC SOE is initialized and finalized as the same at 50%, following the "charge-sustaining" principle [15]. A state transfer function (z) can then be formulated along the timeline, as Eq.

(16). Eq. (16) expresses a function of both power and size of the SC pack, which links EM with sizing and enables the joint optimization.

$$\begin{cases} 0 \le SOC \le 100\% \\ SOE_{min} \le SOE \le 100\% \end{cases} \tag{14}$$

$$\begin{cases} x(k) = SOE(k) \\ SOE(0) = SOE(t_{end}) = 50\% \end{cases} \tag{15}$$

$$z(k) = x(k) - x(k+1) = P_{SC}(k) / E_{SC} / 3.6 \tag{16}$$

(5) Feed objective function of overall costs. With the traversed HESS size and EM strategies as well as the calculated electrical states, the overall costs of HESS over vehicle lifetime can be fulfilled as the objective function (O) in Eq. (17).

$$O = Min \sum_{k=0}^{t_{end}} J_{all}(k) \tag{17}$$

(6) Export results. After completing the above steps, the DP approach would find out the best-case size and EM for the HESS to minimize the overall costs, and the optimization results would be exported. In summary, the brief pseudocodes of the optimization framework are shown in Table 1.

Table 1. Brief pseudocodes of the optimization framework to find the optimal size and EM for the HESS.

% Import profiles %
for $\boldsymbol{E_{BAT}} = \boldsymbol{E_{BAT,min}} : 2\boldsymbol{E_{BAT,min}}$; % battery pack sizing
for $\boldsymbol{E_{SC}} = \boldsymbol{E_{SC,min}} : 10\boldsymbol{E_{SC,min}}$; % SC pack sizing
for $\boldsymbol{k} = 0 : \boldsymbol{t_{end}}$; % timeline of EM
for $\boldsymbol{SOE} = \boldsymbol{SOE_{min}} : 1$; % states of EM
% Calculate electrical states of HESS components %
$\boldsymbol{O} = \text{Min} \sum_{k=0}^{t_{end}} \boldsymbol{J_{all}}(\boldsymbol{k})$; % objective function
end
end
end
end
% Export results %

3. Base-case results

With the proposed HESS sizing method, this section presents the results of a base case. The base case uses the US06 driving cycle [34] and SC/battery HESS topology [18], while other inputs come from the specifications of Tesla Model S P85 EV [35], Panasonic 18650B battery [36] and Maxwell 3400F 2.7V SC [7].

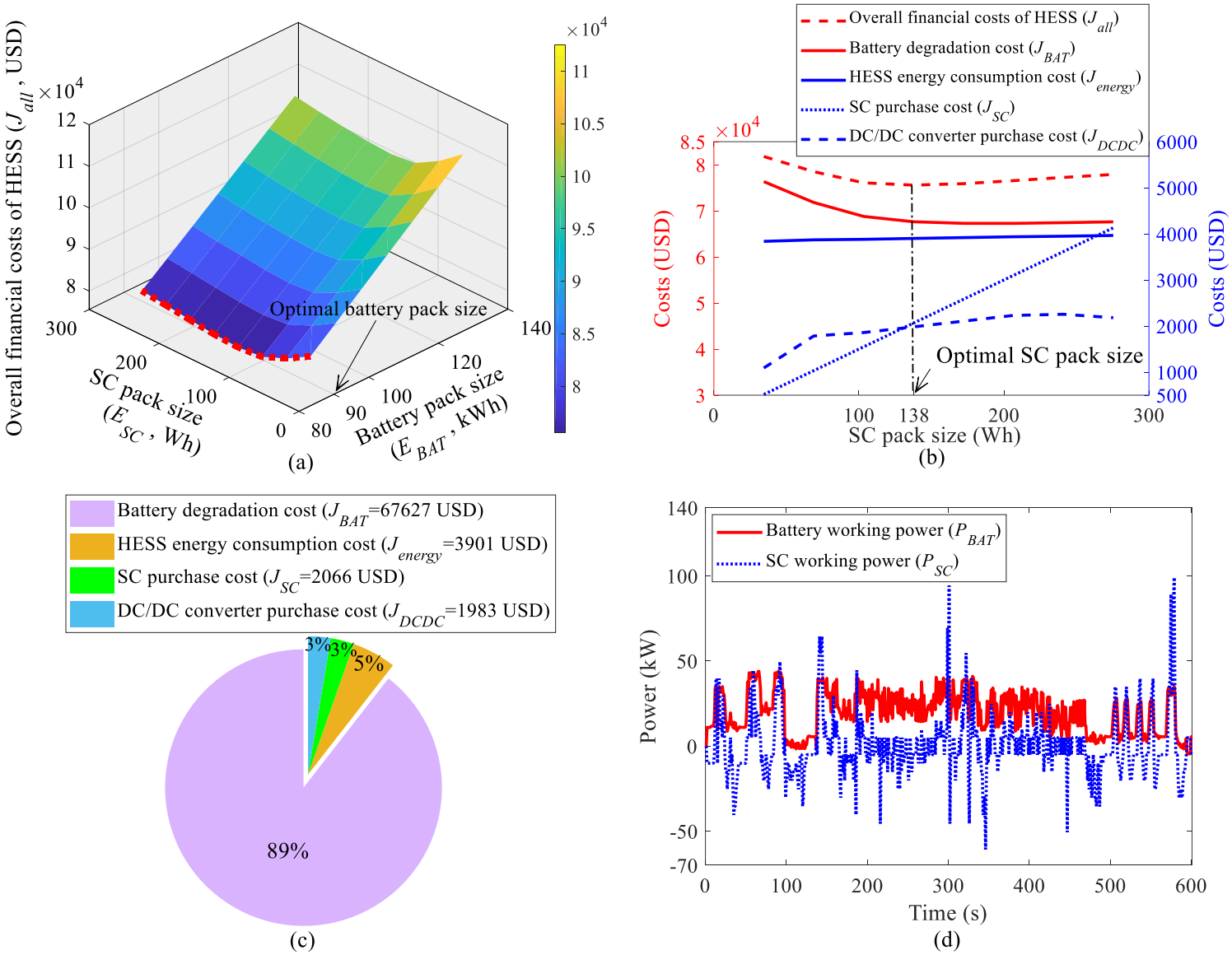

Fig. 3. Optimal sizing and EM results of the base case: (a) Overall costs of HESS with the size of battery pack and SC pack when ensuring EM optimal; (b) Overall costs and four kinds of sub-costs with SC pack size when ensuring both EM and battery pack size optimal; (c) Proportions of sub-costs when ensuring EM, the size of battery and SC pack optimal; (d) Battery working power and SC working power during one US06 driving cycle when ensuring EM, the size of battery and SC pack optimal.

By varying HESS size while ensuring the EM optimal, Fig. 3 (a) shows the overall costs with the size of battery and SC pack. The minimum allowable size of battery pack, as constrained

by Eq. (9), is 90 kWh and highlighted by a red dotted curve. Beyond this curve, the overall costs grow as battery pack size increases. Therefore, the optimal battery pack size is precisely the minimum allowable size. Besides, as SC pack size varies from 0 to 300 Wh, the corresponding overall costs witness a sharp drop firstly, followed by a slow growth. Thus, the optimal SC pack size exists at an extreme point. By varying SC pack size while ensuring the EM and battery pack size optimal, the red dotted curve of overall costs is mapped from Fig. 3 (a) to Fig. 3 (b); four kinds of sub-costs are also plotted. As SC pack size increases, battery degradation cost decreases noticeably at first but finally maintains almost stationary. Therefore, a small SC pack can significantly reduce battery degradation, but a huge SC pack can hardly contribute more. HESS energy consumption cost witnesses a rather slow growth. SC purchase cost increases linearly with SC pack size, while DC/DC converter purchase cost rises rapidly at first but slows down after. In combination of all sub-costs, the overall costs show optimal at the extreme point of SC pack size being 138Wh.

Fig. 3 (c) presents the proportions of sub-costs when both HESS size and EM are held optimal. Battery degradation cost represents 89% of overall costs, which implies that battery degradation is the dominating cause of financial costs and thus needs the most efforts from optimization. HESS energy consumption cost ranks second with a 5% proportion. SC purchase cost and DC/DC converter purchase cost are the initial costs of HESS, but each only makes up 3%, respectively. Thus, most of the overall costs attribute to the long-term costs that happen with HESS operations, while initial costs only represent a tiny proportion. Fig. 3 (d) checks the battery working power and SC working power during one US06 driving cycle when both HESS size and EM are held optimal. In general, the battery pack experiences a discharging process, but its working power is limited to below 50kW. The SC pack works as a power buffer, and its working power fluctuates dramatically between -70kW and 100kW.

4. Sensitivity analysis of different factors

This section sorts out eight sensitive factors and assigns different values to these factors, as Table 2. The characteristics of different types of vehicles can be reflected by using different combinations of factor values. The sensitivity analysis adopts the one-at-a-time (OAT) technique [37], analyzing the influence of one factor on HESS sizing results at a time while keeping the other factors fixed at their base-case values. The definition and values of each factor are explained in the following subsections. Moreover, to investigate whether and why HESS sizing is sensitive to each factor, the evolution of optimal HESS size and overall costs with varying factor values is also analyzed.

Table 2. Eight sensitive factors and their value set used in the sensitivity analysis. (*: base-case values used in Section 3) [32, 38-49]

Sensitive factors			Value set
Vehicle level	Driving cycle		UDDS, HWFET, US06*
	Driving range (km)		142, 284, 426*
System level	HESS topology		SC/battery topology*, battery/SC topology
	Nominal bus voltage (V)		320, 350*, 380
Component level	DC/DC conversion efficiency (%)		84, 88, 92*, 96, 100
	Compon-ent price	Battery (USD/kWh)	100, 200, 300*, 400, 500
		SC (USD/Wh)	5, 10, 15*, 20, 25
		DC/DC converter (USD/kW)	10, 15, 20*, 25, 30

4.1 Vehicle driving cycle

The driving cycle defines the longitudinal speed with time for the EV to follow, based on this, the EV further proposes the energy and power requests for the HESS to fulfill [40]. Standard driving cycles, such as UDDS, HWFET and US06, originate from real-life driving conditions and are typically used for testing the equivalent fuel consumption and the driving range of EV [34]. Therefore, this paper adopts the UDDS, HWFET and US06 driving cycles to investigate the impacts of driving cycles on HESS sizing. The three cycles and the corresponding power demands from the studied Tesla EV are shown in Fig. 4. However, these cycles have different durations and diverse statistic characteristics, which makes it difficult to distinguish which cycle is more intense than the other. In this case, the "intensity factor" is introduced to quantify the intensity of drive cycles. The intensity factor was proposed in Ref. [17] specifically for the EV equipped with a HESS, and the method to recognize the intensity factor is described as follows. One driving cycle can be divided into a few microtrips, which are excursions between two successive instants at which the vehicle speed is zero, e.g., the US06 cycle has five microtrips. The energy demand and peak power of each microtrip can be calculated and used to feed a fuzzy logic algorithm. Based on prescribed membership functions and rules, the fuzzy logic algorithm returns the recognized intensity factor of each microtrip, and the maximum intensity factor of all microtrips can be used as the intensity factor of the driving cycle. Details of the algorithm can be found in [17], while generally, the microtrip with both high energy demand and high peak power tends to be the most intense, while the energy demand has a higher weight than the peak power in determining the intensity factor. With this method, the intensity factors of the UDDS, HWFET and US06 cycles are recognized as 0.257, 0.903 and

0.914, which means that the US06 cycle is the most intense driving cycle while the UDDS cycle is the least intense one for the studied Tesla EV.

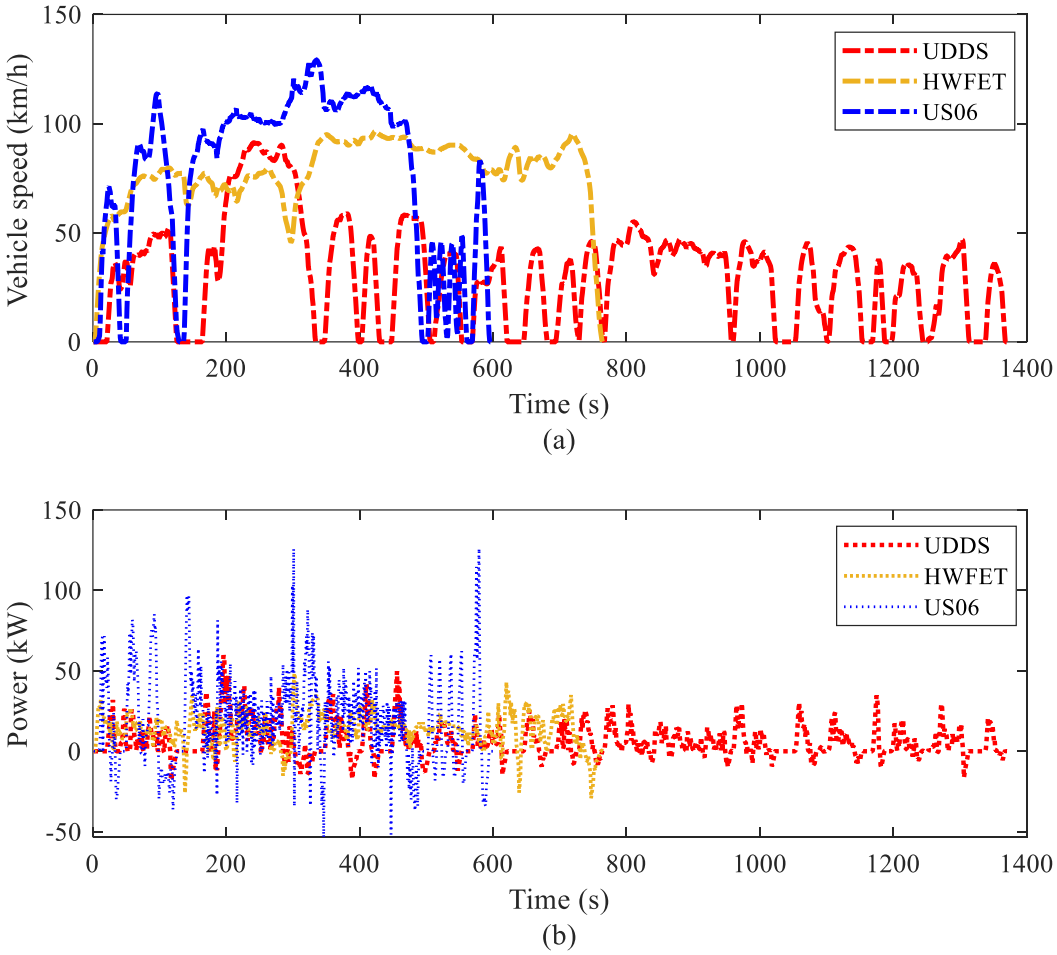

Fig. 4. UDDS, HWFET and US06 drive cycles: (a) vehicle speed with time; (b) power demands from the studied EV.

With the three driving cycles, Fig. 6 (a1) presents the results of optimal overall costs, the size of battery pack and SC pack. As the driving cycle becomes more intense, the optimal overall costs turn increasingly higher, and the US06 cycle has the highest overall costs. The optimal battery pack size remains unchanged at the minimum allowable size since the driving cycle does not change the energy requests for vehicle propulsion, while the optimal SC pack size gets increasingly larger. To understand how the driving cycles cause the above trends, Fig. 6 (a2) presents the energy demand and peak power of the most intense microtrip of each driving cycle. As mentioned previously, the most intense microtrip is the one that determines the intensity factor of the whole driving cycle. Compared with the HWFET cycle, the US06 cycle has a slightly lower energy demand yet a much higher peak power, and the higher peak power results in that the US06 cycle generates more costs and requires a larger SC pack than the

HWFET cycle. Compared with the UDDS cycle, the HWFET cycle has a slightly lower peak power yet a much higher energy demand, and the higher energy demand leads to that the HWFET cycle has more costs and a larger SC pack. It can be seen that the driving cycle with higher peak power does not necessarily raise the overall costs and SC pack size; the energy demand caused by the driving cycle also has an impact, while the driving cycle with both high energy demand and high peak power would lift up the overall costs and SC pack size. Namely, HESS sizing is impacted by the driving cycle with the combined result of both peak power and energy demand.

4.2 Vehicle driving range

The EV driving range is an important vehicle design parameter and a technical specification that is related to the energy capacity of onboard battery pack [39]. Normally, the driving range is designated under standard test procedure. For example, the most widely accepted test procedure is the one issued by US Environmental Protection Agency (EPA), which uses a combination of three standard driving cycles (UDDS, HWFET, US06) to designate the officially recognized driving range [34]. Namely, the driving range is confirmed by the prescribed, particular driving cycles so that it is unaffected by the driving cycles or driving styles adopted for vehicle operation. According to Eq. (9), a longer driving range requires equipping a battery pack with larger energy capacity, which is fulfilled by grouping more parallel branches of battery cells, while the number of serial branches is not affected since the serial voltage of battery pack should maintain the same with that of the bus. The studied Tesla EV specifies the base-case driving range as 426km under the EPA test procedure. This base-case driving range is very long because the studied EV is designed for long-distance driving, while the range of common EVs is normally much shorter at around 200km, but recent years have witnessed the EV driving range being prolonged with the development of new energy storage technologies and EV design standards [39]. Moreover, 142km and 284km, as one-third and two-thirds of the base-case driving range, are assigned into the value set.

The sizing results with different driving ranges are plotted in Fig. 6 (b1). As the driving range increases, the optimal battery pack size experiences a linear growth because the minimum allowable battery pack size linearly grows. Meanwhile, the optimal SC pack size keeps unchanged since the driving range does not change the power requests for vehicle propulsion. The overall costs witness a rapid growth; to find out the reason, the four sub-costs are then checked. It is found that SC purchase cost, DC/DC purchase cost and HESS energy consumption cost witness no much change with growing driving range; however, battery

degradation cost is found increasing noticeably. The increasing battery degradation cost can be explained as follows and validated by Fig. 6 (b2). As abovementioned, the optimal battery pack size grows with growing driving range, which leads to more battery cells being added as parallel branches. In this case, each parallel branch, as well as each battery cell, would share smaller power requests and working current, which relieves the degradation of a single battery cell. In contrast, the entire battery pack, whose degradation accumulates that of every single battery cell, is shown to have an aggravated degradation.

4.3 HESS topology

The HESS topology describes the electrical connections of HESS components. According to the number and position of DC/DC converters, previous research classifies HESS topologies into passive, full-active and semi-active [18]. The semi-active topology, with one single DC/DC converter placed between battery and SC pack, has a good balance between cost and functionality; therefore, it is the most popular practice in engineering. The semi-active topology can be further divided into SC/battery and battery/SC topologies [18], as Fig. 5. Some novel semi-active topologies are also proposed by previous research [44, 45, 50], while these topologies are sort of modifications by adding switches or diodes to the original SC/battery or battery/SC topologies. Therefore, this paper focuses on the original SC/battery and battery/SC topologies, while the former topology is the base case because it is the most popular one in literature [18].

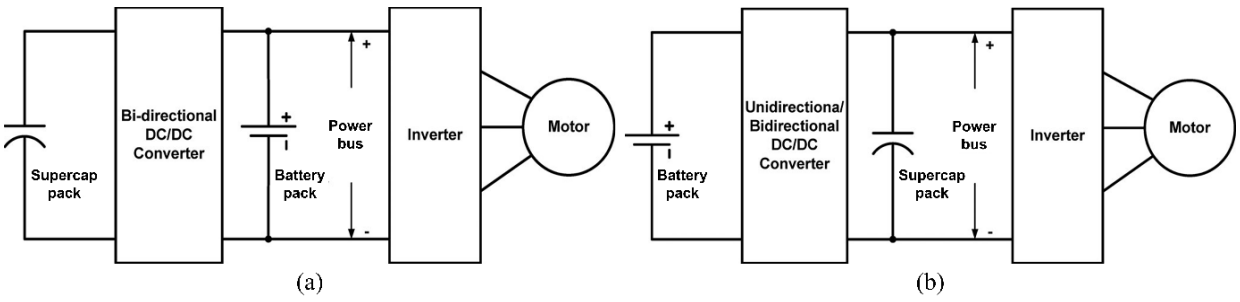

Fig. 5. Semi-active HESS topologies: (a) SC/battery; (b) battery/SC.

The battery/SC topology can be considered as transformed from the SC/battery topology by swapping places of battery and SC pack. However, this swap brings complex influences on the sizing and EM of HESS. Firstly, in the SC/battery topology, the nominal voltage of battery pack has to be the same with the nominal bus voltage since the battery pack is directly connected to the bus, while no hard restriction is enforced to the nominal voltage of SC pack [18]. In contrast, in the battery/SC topology, the nominal voltage of SC pack is required as the

same with that of the bus; consequently, a large number of SCs need to be deployed in series to reach nominal bus voltage, which significantly increases SC purchase cost. Secondly, the operating voltage of SC pack in the SC/battery topology can vary within a broad scope since the DC/DC converter is capable to handle a certain degree of voltage fluctuation [18]. In contrast, in the battery/SC topology, the operating voltage of SC pack cannot vary too much because the voltage fluctuation needs to be handled by the bus; a broad voltage scope of SC pack would impose a challenge on the motor and inverter. To distinguish the voltage scope between SC/battery and battery/SC topologies, this paper considers that the minimum allowable voltage of SC pack for each topology is 20% and 50% of the nominal voltage of SC pack, respectively, while the maximum allowable voltage of SC pack is 100% for both topologies [47]. Thirdly, the voltage scope of SC pack is also related to the ratio of usable energy in the SC pack. Under the voltage scope mentioned above, the usable energy ratio of SC pack for the SC/battery and battery/SC topologies is 96% and 75% [47], respectively. Lastly, the DC/DC converter of SC/battery topology is usually lager than that of battery/SC topology because the maximum working power of SC pack is usually much higher than that of battery pack [19].

Fig. 6 (c1) shows the sizing results with HESS topologies. As the HESS topology changes from SC/battery to battery/SC, the optimal battery pack size does not change, while the optimal SC pack size increases; meanwhile, the usable energy capacity of SC pack grows from 132Wh to 336Wh. The overall costs show a mild growth. By checking the sub-costs, SC purchase cost and HESS energy consumption cost are found increasing while DC/DC converter purchase cost decreasing; however, as analyzed in Fig. 3 (c), these sub-costs each only occupies a small part of overall costs and thus can hardly account for the growth of overall costs. The major reason should attribute to that battery degradation cost is found increasing. To explain the increasing battery degradation cost, the energy throughputs of battery pack and SC pack for both topologies are presented in Fig. 6 (c2). Configured with more usable energy capacity, the SC pack of battery/SC topology has doubled energy throughput than that of SC/battery topology, which contributes to reducing and stabilizing battery power, and consequently lowering the degradation of battery pack. However, Fig. 6 (c2) indicates that the battery pack energy throughput of battery/SC topology is larger than that of SC/battery topology. This is because the battery pack of either topology is responsible for providing the energy required by vehicle propulsion, but in the battery/SC topology, the DC/DC converter interfaces the battery pack and thus the battery pack needs to provide extra energy to cover the DC/DC conversion

losses. In this case, the battery pack of battery/SC topology generates more energy throughput and higher battery degradation.

4.4 Nominal bus voltage

The bus is an intermediary between the mechanical drivetrain and electrical energy storage, conveying power and energy flows between the motor/inverter and the HESS [19]. Practical applications require the nominal voltages of the motor, the HESS and the bus to be as same as possible so that fewer efforts are needed for voltage transformation [43]. For the SC/battery topology, a higher nominal bus voltage requires the battery pack to arrange more battery cells as serial branches but fewer cells as parallel branches. In this case, the equivalent resistance of battery pack would increase while the working current of battery pack can be reduced to fulfill the same power requests. The change of resistance and current would influence battery degradation and HESS energy consumption, while the detailed outcomes need to be checked with results; due to this, the nominal bus voltage is treated as a sensitive factor. The studied EV specifies the base-case nominal bus voltage as 350V. Besides, 380V and 320V are assigned in the value set because they are common nominal voltages of EV motors [46].

Optimal HESS size and overall costs with nominal bus voltage are shown in Fig. 6 (d1). Nominal bus voltage does not influence the optimal battery pack size or SC pack size because it does not change either energy or power requests from vehicle propulsion. The check of sub-costs shows that SC purchase cost, DC/DC converter purchase cost and HESS energy consumption cost do not change too much with increasing nominal bus voltage, but battery degradation cost is significantly reduced, which results in decreasing overall costs. As analyzed previously, a higher bus voltage is beneficial to lowering the working current of the whole battery pack; however, the working current of each battery cell is not necessarily reduced because a higher bus voltage leads to fewer parallel branches to be arranged, which proposes a possibility to increase the working current of battery cells in each parallel branch. By Fig. 6 (d2), it is validated that a higher nominal bus voltage does not much influence the average cell current but can significantly reduce the variance of cell current, which means that cell current is stabilized within a narrower scope centered by the average cell current. In this case, the degradation of single cell is relieved because of the lowered fluctuation of cell current [28]. Since the optimal battery pack size is unchanged with nominal bus voltage, the total number of battery cells in the battery pack is subsequently unchanged. Thus, the reduction of battery cell degradation would eventually lead to the reduction of battery pack degradation.

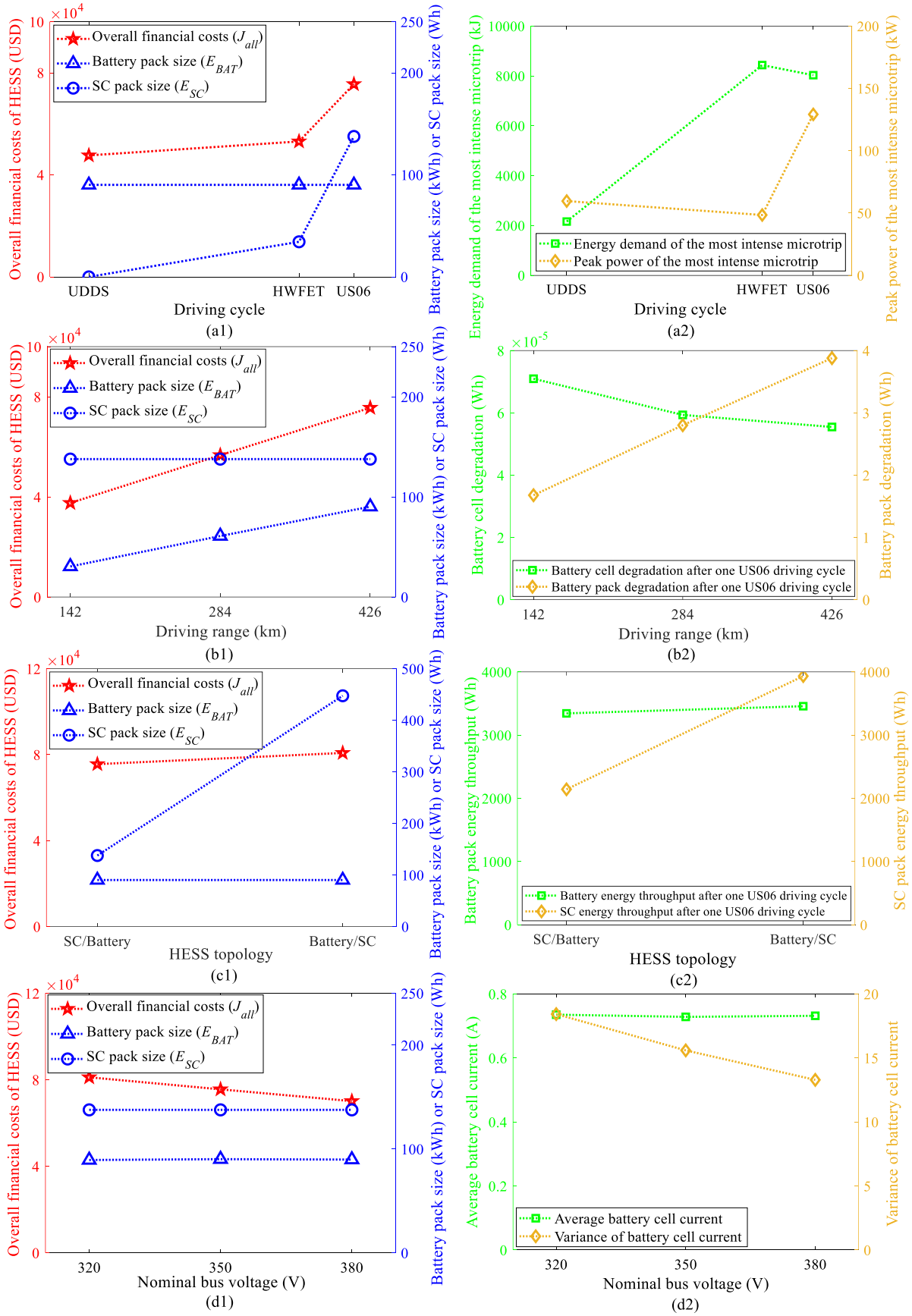

Fig. 6. Optimal overall costs and the corresponding battery pack size and SC pack size with four sensitive factors: (a1) Driving cycle; (b1) Driving range; (c1) HESS topology; (d1) Nominal bus voltage. Explanations for each sensitive factor: (a2) Energy demand and peak power of the most intensive microtrip with driving cycle; (b2) Degradation of battery cell and pack after a single driving cycle with driving range; (c2) Energy throughputs of battery and SC pack after a single driving cycle with HESS topology; (d2) Average and variance of cell current with nominal bus voltage.

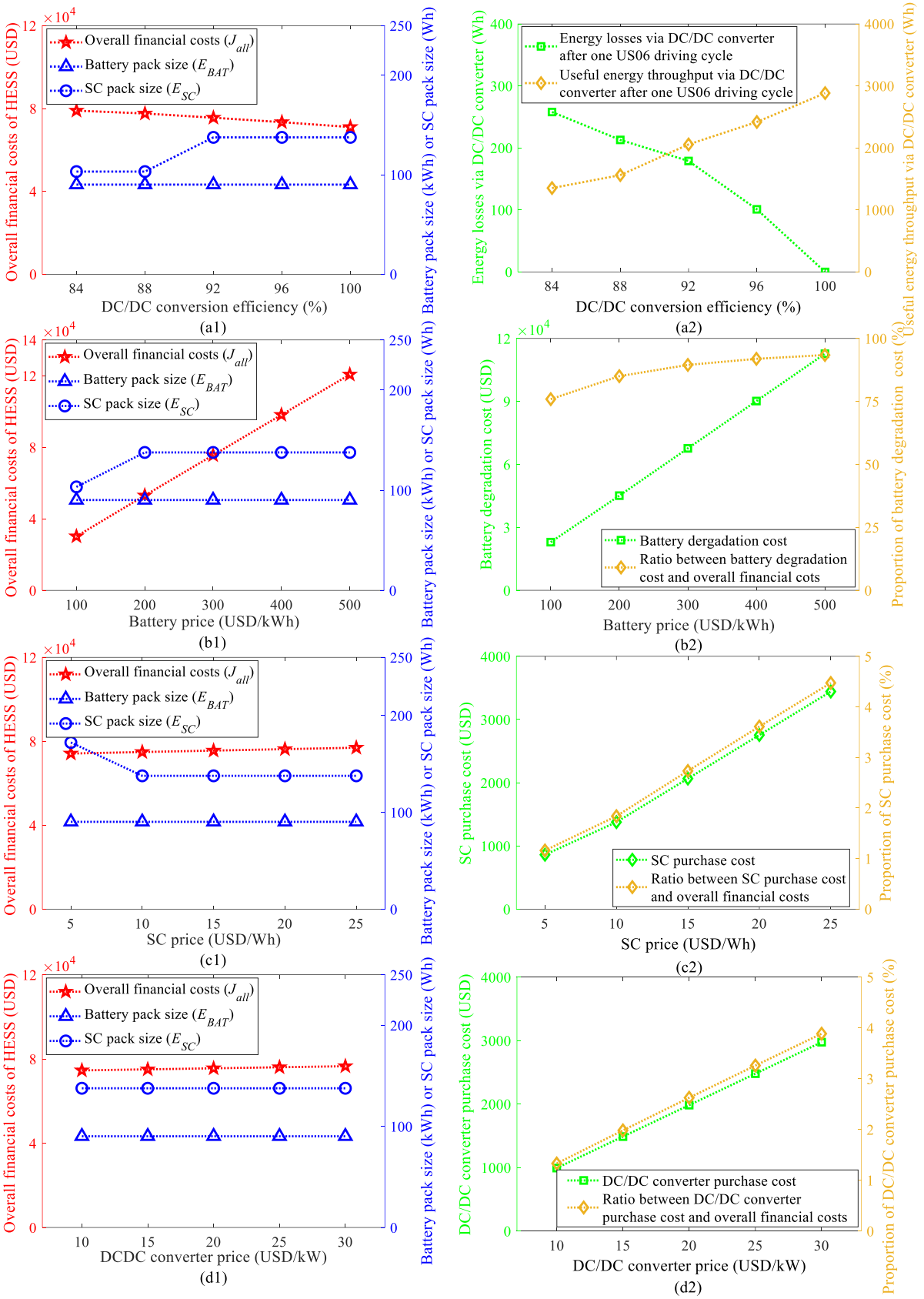

Fig. 7. Optimal overall costs and the corresponding battery pack size and SC pack size with four sensitive factors: (a1) DC/DC conversion efficiency; (b1) Battery price; (c1) SC price; (d) DC/DC converter price. Explanations for each sensitive factor: (a2) Energy losses and useful energy throughput via DC/DC converter with DC/DC conversion efficiency; (b2) Battery degradation cost and its proportion to overall costs with battery price; (c2) SC purchase cost and its proportion to overall costs with SC price; (d2) DC/DC converter purchase cost and its proportion to overall costs with DC/DC converter price.

4.5 DC/DC conversion efficiency

The DC/DC conversion efficiency is defined as the ratio between energy output and energy input [44]. Despite that SCs are commonly considered as energy-efficient storages [48], the effectiveness of SCs also relies on DC/DC conversion efficiency because a lower conversion efficiency results in more energy lost during DC/DC conversion and consequently increased HESS energy consumption. Besides, a lower conversion efficiency also leads to SC energy depleting faster, thus the battery needs to operate more frequently instead of the SC, which increases battery use and leads to aggravated battery degradation. In practical, DC/DC conversion efficiency varies with the input/output voltage and current of DC/DC converter [49]. However, in order to find out the straight relationship between DC/DC conversion efficiency and HESS sizing, the conversion efficiency is assigned as constants from 84% to 100% with a 4% interval, while 92% is used in the base case.

Fig. 7 (a1) presents the results with DC/DC conversion efficiency. As the efficiency grows, the overall costs witness a near-linear decline. This decline can be attributed to the reduction of HESS energy consumption and battery degradation, which can be validated by Fig. 7 (a2). With increasing DC/DC conversion efficiency, the energy losses due to DC/DC conversion are greatly reduced; thus, the HESS energy consumption to fulfill vehicle propulsion is then reduced. Fig. 7 (a2) also indicates that more useful energy throughput arises via DC/DC converter. This means that the SC pack is better exploited by buffering more energy and power, which relieves the workloads of battery pack, so that battery degradation can be significantly lowered. Besides, the optimal SC pack size finds an increasing tendency with improving conversion efficiency. This can be explained as, with more efficient DC/DC conversion, more SCs are encouraged to be configured; despite the increasing SC purchase cost, the benefit of reducing battery degradation cost and HESS energy consumption cost outweighs the incremental SC purchase cost.

4.6 Component price

It is easy to understand that as the component price becomes higher, the overall costs would increase, and the component would be downsized. As formulated in Eqs. (1), (2) and (3), this paper considers the prices of three kinds of HESS components: battery, SC and DC/DC converter, and assigns the value sets in Table 2. The results of overall costs and HESS size with battery price, SC price, DC/DC converter price are provided in Figs. 7 (b1), (c1) and (d1); the corresponding explanations are offered in Figs. 7 (b2), (c2) and (d2), respectively. Fig. (b1) shows that the increasing battery price leads to the overall costs growing dramatically, while

battery degradation cost represents an increasingly high proportion of overall costs, and this proportion reaches 93% when battery price is 500 USD/kWh, as shown in Fig. 7 (b2). The increasing battery price also leads to a tendency to raise the optimal SC pack size, as Fig. 7 (b1). This can be explained as, with increasing battery price, reducing battery degradation cost becomes a more crucial matter; thus, more SCs are demanded to help reduce battery degradation. As SC price or DC/DC converter price increases, the overall costs witness a slow rise, because either SC purchase cost or DC/DC converter purchase cost only represents around 3% of overall costs, as Figs. 7 (c2) and (d2). Besides, the optimal SC pack size shows a decreasing tendency with SC price, in which case the incremental SC purchase cost outweighs the reduced battery degradation cost and thus discourages more SCs from being configured. In contrast, the DC/DC converter price has no evident influence on the optimal SC pack size.

5. Impact degrees of different factors

Following the sensitivity analysis, this section quantifies the relative importance of each sensitive factor as an impact degree. The impact degrees of different factors are compared and discussed in terms of practical engineering.

5.1 Quantification of impact degree

By referring to the discipline of mathematical finance, this section firstly introduces the quantification of "sensitivity" [51], as Eq. (18). This equation calculates the percentage change of both output and input compared to the base case, and obtains the sensitivity by dividing the former percentage change by the later one. In this paper, the input is one of the factor values assigned in Table 2, while the output is the corresponding overall costs. For each value (except the base-case value) of one sensitive factor, a nonzero sensitivity can be worked out. Finally, the impact degree of that sensitive factor is quantified as the average of all nonzero sensitivities, as Eq. (19), where n represents the number of non-base-case values. When calculating the impact degrees of driving cycle and HESS topology, Eq. (18) cannot be directly used because the value sets of driving cycle and HESS topology are not numerical. For calculating the impact degree of driving cycle, the intensity factor of the driving cycle is adopted as the input into Eq. (18); while for calculating the impact degree of HESS topology, SC pack energy capacity is adopted because it is the most remarkable difference between different HESS topologies in terms of HESS sizing [18].

$$Sensitivity = \left| \frac{\%\ Change\ in\ output}{\%\ Change\ in\ input} \right| \tag{18}$$

$$Impact\ degree = \frac{\sum_{i=1}^{n} Sensitivity_i}{n} \tag{19}$$

5.2 Comparison of impact degrees of different factors

The impact degrees of eight sensitive factors are worked out as the radar plot in Fig. 8. The driving cycle shows the largest impact degree - 1.243 and is considered to have a big impact on HESS overall costs. The driving cycle is not only a design parameter prescribing vehicle driving conditions but somewhat a reflection of driving habits [40]. From the standpoint of the driver, less aggressive driving habits such as low-speed cruise and mild acceleration can significantly reduce the overall costs of HESS.

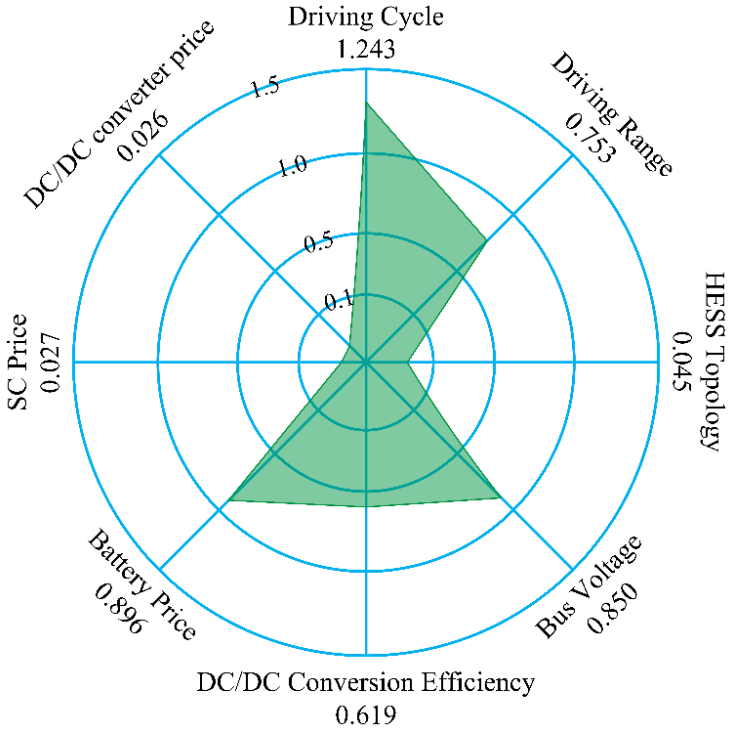

Fig. 8. Radar plot of the impact degrees of eight sensitive factors. The number under each sensitive factor represents the corresponding impact degree.

The battery price, bus voltage, driving range and DC/DC conversion efficiency have descending impact degrees from 0.896 to 0.619, and they are considered to have medium impacts on HESS overall costs. Currently, the battery price is still high [52]; therefore, even a small percentage of battery degradation could bring a huge battery degradation cost, while the reduction of battery price relies on the breakthrough of economical battery manufacturing technology. The nominal bus voltage affects the overall costs by changing the electrical configuration of battery pack, while a higher bus voltage can better reduce overall costs. As

compared with lowering battery price, boosting nominal bus voltage is more practicable to achieve, but this relies on a good match with the motor and inverter [43]. The driving range is an EV design parameter related to the battery pack size. Nowadays, the concern of "range-anxiety" is pushing EV manufacturers to deploy an increasingly larger battery pack to fulfill a longer driving range [39]. However, as the battery pack becomes larger with increasing driving range, the over costs are found growing rapidly due to the fast-rising battery degradation cost. The DC/DC conversion efficiency determines not only the energy conversion losses but also the effectiveness of SC pack, while the improvement of DC/DC conversion efficiency would require efforts on developing efficient topologies and power electronics [44].

The HESS topology, SC price and DC/DC converter price have descending impact degrees from 0.045 to 0.026, and they are considered to have little impacts on overall costs. Although HESS topology can change the electrical connections of HESS components, it is found to have no much impact on overall costs. The SC price is normally much higher than the battery price [19], but this does not mean that SC price has a bigger impact than battery price. This is because the optimal sizing results suggest configuring a small SC pack due to the fact that the efficacy of reducing battery degradation becomes increasingly less effective with more SCs being deployed. Therefore, the SC purchase cost only makes up around 3% of the overall costs. The DC/DC converter price has the least impact on overall costs; thus, it would be the last factor to consider when designing a HESS.

To offer general HESS sizing guides for EV applications, Table 3 summaries the trends of optimal battery pack size, SC pack size and overall costs with eight sensitive factors, plus the impact degree of each factor.

Table 3. Trends of optimal battery pack size, SC pack size and HESS overall costs with eight sensitive factors increasing, plus the impact degree of each factor.
(↑:increase, ↓:decrease, ─:unaffected)

	Driving cycle	Driving range	HESS topology	Bus voltage	DC/DC efficiency	Battery price	SC price	DC/DC price
Battery size	─	↑	─	─	─	─	─	─
SC size	↑	─	↑	─	↑	↑	↓	─
Overall costs	↑	↑	↑	↓	↓	↑	↑	↑
Impact degree	High	medium	low	medium	medium	medium	low	low

6. Conclusion

This paper focuses on optimizing the vehicle-lifetime costs of battery-SC HESS by formulating a sizing problem with consideration of sensitivity analysis. An optimization framework is proposed based on the DP approach to solve both the optimal HESS size and EM strategies. Eight parameters of the EV, HESS and components are used as sensitive factors by discussing the trends of optimal HESS size and costs with varying factor values. The relative importance of each factor is quantified as an impact degree and discussed in terms of practical engineering. The following conclusion is obtained as general sizing guides for HESS in EV applications.

(1) Size of battery pack and SC pack: The HESS should deploy an as small as possible battery pack, as long as the vehicle driving range can be guaranteed. The SC pack size is a U-shape function of HESS costs so that there is an optimal SC pack size at which the HESS costs can be minimized.

(2) Proportions of HESS costs: Battery degradation is the dominating cause (more than 75%) of HESS costs so that it needs the most attention when sizing a HESS. In contrast, the energy consumption of HESS and the initial costs to purchase the SC pack and DC/DC converter only represent a small part (around 11%) of HESS costs.

(3) Impacts of sensitive factors: Vehicle driving cycle has the biggest impact on HESS costs since an intense driving cycle proposes both high peak power and high energy demand for the HESS to fulfill. When sizing a HESS for EVs designed with high acceleration capabilities or for drivers with aggressive driving styles, the SC pack needs to be significantly enlarged. Battery price, nominal bus voltage, vehicle driving range and DC/DC conversion efficiency have medium impacts on HESS costs. The currently high battery price determines that even a small percentage of battery degradation leads to a huge battery degradation cost, while the tendency of increasingly economical battery technologies would enable the SC pack to be downsized. The nominal bus voltage affects the electrical configuration and equivalent circuit parameters of the battery pack, and a high nominal bus voltage can lower the fluctuation of battery cell current and thus reduce battery degradation and HESS costs. Although boosting nominal bus voltage seems like a convenient, practicable approach to reduce HESS costs, the coordination of bus voltage with the motor and inverter must be settled simultaneously. Vehicle driving range is directly related to the energy capacity of battery pack. Demands of long driving range require to upsize the battery pack, but a large battery pack can generate more battery degradation cost and HESS costs. DC/DC conversion efficiency determines the effectiveness

of SC pack. As the conversion efficiency improves, the SC pack can become larger and thus better reduce battery degradation without increasing the total HESS costs. HESS topology, SC price and DC/DC converter price have little impacts on HESS costs so that they should be considered with low priorities in practical engineering. Although HESS topology notably affects the SC pack size, the HESS costs are not obviously influenced by it. Compared with battery price, the prices of SC and DC/DC converter have much smaller impacts on HESS costs and size, because the purchase costs of SC pack and DC/DC converter are much less than battery degradation cost.

Acknowledgements

The first author gratefully acknowledges the financial supports from China Scholarship Council and University of Southampton.

Appendix

The state-space representation of the HESS is expressed as Eqs. (A1) to (A6), and the parameters are declared by the nomenclature in Table A1. The HESS is considered as the combination of a battery pack, a SC pack and a DC/DC converter, using the topology in Fig. 5 (a). The battery/SC is a charge reservoir and an equivalent circuit whose parameters are a piecewise linear function of the SOC and temperature, defined by empirical data. The equivalent circuit of the battery/SC is a voltage source/capacitance in series with an internal resistance. The conversion efficiency of DC/DC converter accounts for the power loss during the SC being interfaced by the DC/DC converter. The total power of HESS is the useful power from/to both battery pack and SC pack.

$$\begin{bmatrix} U_{BAT} \\ U_{SC} \end{bmatrix} = \begin{bmatrix} U_{oc,BAT} \\ U_{oc,SC} \end{bmatrix} + \begin{bmatrix} I_{BAT} & 0 \\ 0 & I_{SC} \end{bmatrix} \begin{bmatrix} -R_{BAT} \\ -R_{SC} \end{bmatrix} \tag{A1}$$

$$\begin{bmatrix} U_{oc,BAT} \\ \dot{U}_{oc,SC} \end{bmatrix} = \begin{bmatrix} f(SOC) \\ \dfrac{I_{BAT}}{C_{SC}} \end{bmatrix} \tag{A2}$$

$$\begin{bmatrix} R_{BAT} \\ R_{SC} \end{bmatrix} = \begin{bmatrix} g(SOC, T_{BAT}) \\ h(T_{SC}) \end{bmatrix} \tag{A3}$$

$$\begin{bmatrix} \dot{SOC} \\ \dot{SOE} \end{bmatrix} = \begin{bmatrix} -\frac{1}{3600}\frac{I_{BAT}}{C_{BAT}} \\ -\frac{P_{SC}}{3.6E_{SC}} \end{bmatrix} \tag{A4}$$

$$\begin{bmatrix} P_{BAT} \\ P_{SC} \end{bmatrix} = \begin{bmatrix} U_{BAT} & 0 \\ 0 & U_{SC} \end{bmatrix} \begin{bmatrix} I_{BAT} \\ I_{SC} \end{bmatrix} \tag{A5}$$

$$P_{HESS} = P_{BAT} + P_{SC} \begin{bmatrix} \eta_{DCDC} \\ \frac{1}{\eta_{DCDC}} \end{bmatrix} \begin{matrix} ,P_{SC} \geq 0 \\ ,P_{SC} < 0 \end{matrix} \tag{A6}$$

Table A1. Nomenclature for the state-space representation of HESS

C_{BAT}	Capacity of battery pack, *Ah*	SOC	State of charge of battery pack, *%*
C_{SC}	Capacitance of SC pack, *F*	SOE	State of energy of SC pack, *%*
E_{SC}	Energy capacity of SC pack, *Wh*	T_{BAT}	Battery pack temperature, *K*
I_{BAT}	Battery pack current, *A*	T_{SC}	SC pack temperature, *K*
I_{SC}	SC pack current, *A*	U_{BAT}	Battery pack voltage, *V*
P_{BAT}	Battery pack power, *kW*	U_{SC}	SC pack voltage, *V*
P_{SC}	SC pack power, *kW*	$U_{oc,BAT}$	Battery pack open-circuit voltage, *V*
P_{HESS}	HESS power, *kW*	$U_{oc,SC}$	SC pack open-circuit voltage, *V*
R_{BAT}	Internal resistance of battery pack, *Ohm*	η_{DCDC}	DC/DC conversion efficiency, *%*
R_{SC}	Internal resistance of SC pack, *Ohm*		

References

[1] Berckmans G, Messagie M, Smekens J, Omar N, Vanhaverbeke L, Van Mierlo J. Cost projection of state of the art lithium-ion batteries for electric vehicles up to 2030. Energies. 2017;10(9):1314.
[2] Yang B, Zhu T, Zhang X, Wang J, Shu H, Li S, et al. Design and implementation of Battery/SMES hybrid energy storage systems used in electric vehicles: A nonlinear robust fractional-order control approach. Energy. 2019:116510.
[3] Song Z, Hofmann H, Li J, Hou J, Han X, Ouyang M. Energy management strategies comparison for electric vehicles with hybrid energy storage system. Applied Energy. 2014;134:321-31.
[4] Esmaeili S, Anvari-Moghaddam A, Jadid S. Optimal operation scheduling of a microgrid incorporating battery swapping stations. IEEE Transactions on Power Systems. 2019;34(6):5063-72.
[5] Wang Y, Sun Z, Chen Z. Development of energy management system based on a rule-based power distribution strategy for hybrid power sources. Energy. 2019;175:1055-66.
[6] Ostadi A, Kazerani M. A comparative analysis of optimal sizing of battery-only, ultracapacitor-only, and battery–ultracapacitor hybrid energy storage systems for a city bus. IEEE Transactions on Vehicular Technology. 2014;64(10):4449-60.
[7] Datasheet of 2.7V 3400F Ultracapacitor Cell. Maxwell Technologies Inc.; 2018.
[8] Gomozov O, Trovão JPF, Kestelyn X, Dubois MR. Adaptive energy management system based on a real-time model predictive control with nonuniform sampling time for multiple energy storage electric vehicle. IEEE Transactions on Vehicular Technology. 2016;66(7):5520-30.
[9] Zhang L, Hu X, Wang Z, Sun F, Deng J, Dorrell DG. Multiobjective optimal sizing of hybrid energy storage system for electric vehicles. IEEE Transactions on Vehicular Technology. 2017;67(2):1027-35.
[10] Eldeeb HH, Elsayed AT, Lashway CR, Mohammed O. Hybrid energy storage sizing and power splitting optimization for plug-in electric vehicles. IEEE Transactions on Industry Applications. 2019;55(3):2252-62.
[11] Shen J, Dusmez S, Khaligh A. Optimization of Sizing and Battery Cycle Life in Battery/Ultracapacitor Hybrid Energy Storage Systems for Electric Vehicle Applications. IEEE Transactions on Industrial Informatics. 2014;10(4):2112-21.
[12] Zhang L, Hu X, Wang Z, Sun F, Deng J, Dorrell DG. Multiobjective Optimal Sizing of Hybrid Energy Storage System for Electric Vehicles. IEEE Transactions on Vehicular Technology. 2018;67(2):1027-35.
[13] Masih-Tehrani M, Ha'iri-Yazdi M-R, Esfahanian V, Safaei A. Optimum sizing and optimum energy management of a hybrid energy storage system for lithium battery life improvement. Journal of Power Sources. 2013;244:2-10.
[14] Song Z, Li J, Hou J, Hofmann H, Ouyang M, Du J. The battery-supercapacitor hybrid energy storage system in electric vehicle applications: A case study. Energy. 2018;154:433-41.
[15] Song Z, Hofmann H, Li J, Han X, Ouyang M. Optimization for a hybrid energy storage system in electric vehicles using dynamic programing approach. Applied Energy. 2015;139:151-62.
[16] Yu H, Tarsitano D, Hu X, Cheli F. Real time energy management strategy for a fast charging electric urban bus powered by hybrid energy storage system. Energy. 2016;112:322-31.
[17] Song Z, Hou J, Xu S, Ouyang M, Li J. The influence of driving cycle characteristics on the integrated optimization of hybrid energy storage system for electric city buses. Energy. 2017;135:91-100.
[18] Cao J, Emadi A. A New Battery/UltraCapacitor Hybrid Energy Storage System for Electric, Hybrid, and Plug-In Hybrid Electric Vehicles. IEEE Transactions on Power Electronics. 2012;27(1):122-32.
[19] Ehsani M, Gao Y, Longo S, Ebrahimi K. Modern electric, hybrid electric, and fuel cell vehicles: CRC press, 2018.
[20] Song Z, Hou J, Hofmann HF, Lin X, Sun J. Parameter identification and maximum power estimation of battery/supercapacitor hybrid energy storage system based on Cramer–Rao bound analysis. IEEE Transactions on Power Electronics. 2018;34(5):4831-43.
[21] Zhang L, Hu X, Wang Z, Sun F, Dorrell DG. A review of supercapacitor modeling, estimation, and applications: A control/management perspective. Renewable and Sustainable Energy Reviews. 2018;81:1868-78.
[22] Lu L, Han X, Li J, Hua J, Ouyang M. A review on the key issues for lithium-ion battery management in electric vehicles. Journal of Power Sources. 2013;226:272-88.

[23] Liu C, Wang Y, Chen Z. Degradation model and cycle life prediction for lithium-ion battery used in hybrid energy storage system. Energy. 2019;166:796-806.
[24] Samadani E, Mastali M, Farhad S, Fraser RA, Fowler M. Li-ion battery performance and degradation in electric vehicles under different usage scenarios. International Journal of Energy Research. 2016;40(3):379-92.
[25] Carignano M, Roda V, Costa-Castelló R, Valiño L, Lozano A, Barreras F. Assessment of energy management in a fuel cell/battery hybrid vehicle. IEEE access. 2019;7:16110-22.
[26] Mamun A-A, Liu Z, Rizzo DM, Onori S. An integrated design and control optimization framework for hybrid military vehicle using lithium-ion battery and supercapacitor as energy storage devices. IEEE Transactions on Transportation Electrification. 2018;5(1):239-51.
[27] Wang J, Purewal J, Liu P, Hicks-Garner J, Soukazian S, Sherman E, et al. Degradation of lithium ion batteries employing graphite negatives and nickel–cobalt–manganese oxide + spinel manganese oxide positives: Part 1, aging mechanisms and life estimation. Journal of Power Sources. 2014;269:937-48.
[28] Zhu T, Min H, Yu Y, Zhao Z, Xu T, Chen Y, et al. An Optimized Energy Management Strategy for Preheating Vehicle-Mounted Li-ion Batteries at Subzero Temperatures. Energies. 2017;10(2):243.
[29] Li J, Gee AM, Zhang M, Yuan W. Analysis of battery lifetime extension in a SMES-battery hybrid energy storage system using a novel battery lifetime model. Energy. 2015;86:175-85.
[30] Kreczanik P, Venet P, Hijazi A, Clerc G. Study of supercapacitor aging and lifetime estimation according to voltage, temperature, and RMS current. IEEE Transactions on industrial electronics. 2014;61(9):4895-902.
[31] Peng J, He H, Xiong R. Rule based energy management strategy for a series–parallel plug-in hybrid electric bus optimized by dynamic programming. Applied Energy. 2017;185:1633-43.
[32] Chen Z, Xiong R, Wang C, Cao J. An on-line predictive energy management strategy for plug-in hybrid electric vehicles to counter the uncertain prediction of the driving cycle. Applied Energy. 2017;185:1663-72.
[33] Zhang S, Xiong R, Sun F. Model predictive control for power management in a plug-in hybrid electric vehicle with a hybrid energy storage system. Applied Energy. 2017;185:1654-62.
[34] T J Barlow SL, I S McCrae and PG Boulter. A reference book of driving cycles for use in the measurement of road vehicle emissions. Published Project Report. 3 ed: TRL Limited; 2009.
[35] Vynakov O, Savolova E, Skrynnyk A. Modern electric cars of Tesla Motors company. Automation of technological and business-processes. 2016(Volume 8):9-18.
[36] Kamalisiahroudi S, Huang J, Li Z, Zhang J. Study of temperature difference and current distribution in parallel-connected cells at low temperature. Int J Electr Comput Energ Electron Commun Eng. 2014;8(10):1471-4.
[37] Luta DN, Raji AK. Optimal sizing of hybrid fuel cell-supercapacitor storage system for off-grid renewable applications. Energy. 2019;166:530-40.
[38] Yan X, Fleming J, Allison C, Lot R. Portable Automobile Data Acquisition Module (ADAM) for naturalistic driving study. 15th European Automotive Congress2017.
[39] Patzak A, Bachheibl F, Baumgardt A, Dajaku G, Moros O, Gerling D. Driving range evaluation of a multi-phase drive for low voltage high power electric vehicles. Conference Driving range evaluation of a multi-phase drive for low voltage high power electric vehicles. IEEE, p. 1-7.
[40] Huang X, Tan Y, He X. An intelligent multifeature statistical approach for the discrimination of driving conditions of a hybrid electric vehicle. IEEE Transactions on Intelligent Transportation Systems. 2011;12(2):453-65.
[41] Zhang S, Xiong R. Adaptive energy management of a plug-in hybrid electric vehicle based on driving pattern recognition and dynamic programming. Applied Energy. 2015;155:68-78.
[42] Xu Q, Xiao J, Hu X, Wang P, Lee MY. A Decentralized Power Management Strategy for Hybrid Energy Storage System With Autonomous Bus Voltage Restoration and State-of-Charge Recovery. IEEE Transactions on Industrial Electronics. 2017;64(9):7098-108.
[43] Ma Y, Lin H, Wang Z, Wang T. Capacitor voltage balancing control of modular multilevel converters with energy storage system by using carrier phase-shifted modulation. Conference Capacitor voltage balancing control of modular multilevel converters with energy storage system by using carrier phase-shifted modulation. p. 1821-8.

[44] Lai C, Cheng Y, Hsieh M, Lin Y. Development of a Bidirectional DC/DC Converter With Dual-Battery Energy Storage for Hybrid Electric Vehicle System. IEEE Transactions on Vehicular Technology. 2018;67(2):1036-52.
[45] Zhang Y, Cheng X-F, Yin C, Cheng S. A Soft-switching Bidirectional DC-DC Converter for the Battery Super-capacitor Hybrid Energy Storage System. IEEE Transactions on Industrial Electronics. 2018.
[46] Pellegrino G, Vagati A, Boazzo B, Guglielmi P. Comparison of Induction and PM Synchronous Motor Drives for EV Application Including Design Examples. IEEE Transactions on Industry Applications. 2012;48(6):2322-32.
[47] Min H, Lai C, Yu Y, Zhu T, Zhang C. Comparison Study of Two Semi-Active Hybrid Energy Storage Systems for Hybrid Electric Vehicle Applications and Their Experimental Validation. Energies. 2017;10(3):279.
[48] Lystianingrum V, Agelidis VG, Hredzak B. State of health and life estimation methods for supercapacitors. Conference State of health and life estimation methods for supercapacitors. IEEE, p. 1-7.
[49] Zhao W, Wu G, Wang C, Yu L, Li Y. Energy transfer and utilization efficiency of regenerative braking with hybrid energy storage system. Journal of Power Sources. 2019;427:174-83.
[50] Song Z, Zhang X, Li J, Hofmann H, Ouyang M, Du J. Component sizing optimization of plug-in hybrid electric vehicles with the hybrid energy storage system. Energy. 2018;144:393-403.
[51] Borgonovo E, Gatti S, Peccati L. What drives value creation in investment projects? An application of sensitivity analysis to project finance transactions. European Journal of Operational Research. 2010;205(1):227-36.
[52] Ruan J, Song Q, Yang W. The application of hybrid energy storage system with electrified continuously variable transmission in battery electric vehicle. Energy. 2019;183:315-30.